Differences Changes in Cerebellar Functional Connectivity of Parkinson's patients with visual hallucinations

Liangcheng Qu , Chuan Liu , Yiting Cao , Kuiying Yin * , Weiguo Liu * , Jingping Shi *

Posted Date: 25 September 2023

doi: 10.20944/preprints202309.1618.v1

Keywords: Parkinson's disease; visual hallucinations; cerebellum; functional connectivity

Article

Differences Changes in Cerebellar Functional Connectivity of Parkinson's Patients with Visual Hallucinations

Liangcheng Qu [1], Chuan Liu [1], Yiting Cao [2], KuiYing Yin [1,*], WeiGuo Liu [2,*] and JingPing Shi [2,*]

[1] Link Sense Laboratory, Nanjing Research Institute of Electronic Technology, Nanjing 210019, China
[2] Department of Geriatrics, Affiliated Brain Hospital of Nanjing Medical University, Nanjing, 210029, China
* Correspondence: yinkuiying77@outlook.com; liuweiguo111@sina.com; profshijp@163.com;

Abstract: Recent studies have discovered that functional connections are impaired in patients with Parkinson's disease (PD) accompanied by hallucinations(PD-H), even at the preclinical stage. The cerebellum has been implicated as playing a role in cognitive processes. However, the functional connectivity (FC) between cognitive sub-regions of the cerebellum of PD patients with hallucinations needs to be further clarified. Resting-state functional magnetic resonance imaging (rs-fMRI) data from three groups (17 PD-H, 13 no hallucinations accompanying the (PD-NH), and 26 healthy controls (HC)) was collected in this study to explore the role of cerebellar FC changes in the cognitive performance. Additionally, we define cerebellar FC as a training feature for classifying all subjects using Support Vector Machine(SVM). We found that PD-H patients' cerebellum(Vermis_4_5) FC had increased within the left side of the precuneus(PCUN) compared to HC, cerebellum(Vermis_1_2) had increased within bilateral opercular part of the inferior frontal gyrus(IFGoprec) and triangular part of the inferior frontal gyrus(IFCtriang), left side of postcentral gyrus(PoCG), Inferior parietal lobe(IPL), and PCUNs compared to PD-NH. In the training results of machine learning, cerebellar FC has also been proven to be an effective biomarker feature, with a recognition rate of over 90% for PD-H. These findings indicate that cortico-cerebellar FC in PD-H and PD-NH patients were significantly disrupted with different distributions. The proposed pipeline offers a promising low-cost alternative for the diagnosis of preclinical PD-H and can be useful for other degenerative brain disorders.

Keywords: Parkinson's disease; visual hallucinations; cerebellum; functional connectivity

1. Introduction

PD is a common and complex degenerative disease of the central nervous system in middle-aged and older people, and its main pathological change is the loss of dopaminergic neurons in the dense part of the substantia nigra of the midbrain; clinically, it mainly presents with motor symptoms such as bradykinesia, resting tremor, and postural instability, as well as various non-motor symptoms[1]. The non-motor symptoms include autonomic, cognitive dysfunction, psychiatric disorders, sleep disorders, and sensory symptoms[2]. Hallucinations are a common psychiatric symptom, including visual, auditory, and olfactory hallucinations, among which visual hallucinations are the most common, with more than 40% of PD patients experiencing visual hallucinations, and this percentage increases to 80% as the disease progresses[3]. Visual hallucinations seriously reduce the quality of life of PD patients and increase the rate of hospitalization and death and the burden on caregivers [4,5].

Many PD patients have fast-eye movement sleep disorders that manifest as vivid dreams or just optical illusions (a concept included in minor hallucinations). Whether or not the patient is hallucinating requires a careful history and the nature of the content of the hallucinations. A broader scale is currently available, but scale scores are subject to bias due to various factors.

Resting-state functional magnetic resonance imaging (rs-fMRI) is an in vivo functional imaging technique, which measures blood oxygen level-dependent (BOLD) signals when scanning subjects at natural rest without any explicit task involvement. It is widely used in the diagnosis and prediction

 doi:10.20944/preprints202309.1618.v1

of the disease progression of PD [6]. The application of resting-state fMRI techniques has revealed imaging features of PD concerning brain structure[7]. Studies have shown that FC in PD are impaired as early as the early stages of hallucinatory concomitant[8], Holroyd found higher activation in the frontal and subcortical lobes and lower activation in the visual cortex during visual stimulation in patients with concomitant visual hallucinations, suggesting that PD patients with visual hallucinations are less responsive to external visual stimuli[9]; Yao et al. used a combined VBM and FC resting Yao et al. used a combined VBM and FC resting-state fMRI study to find no significant reduction in gray matter volume, but a significant increase in DMN activation compared to patients without hallucinations[10].

Recent studies have implicated the role of the cerebellum in cognitive processes [11–13]. Cerebellar cognitive affective syndrome (CCAS) is characterized by executive dysfunction, spatial cognitive impairment, language deficits, and personality changes [14–18]. The human cerebellar cortex is a complicated structure, as the surface of is more tightly folded than the cerebral cortex and has almost 80% of the surface area of the neocortex. The nerve fiber connections to the brain's cognitive network are extensive[19], indicating that the cerebellum plays a vital role in the evolution of behavior and cognition. Lower GMV(grey matter volume) was found within cerebellar lobule VIIIb, VIIIa, IX, VIIb, predominantly within PD[20].

Many imaging studies have confirmed that cerebellar FC are associated with cognitive networks [21-23], particularly with the DMN[24]. The posterior cerebellum (i.e., lobule VI-Crus I, lobule Crus II-VIIB, and lobule IX) is critical for cognitive representation[25–27]. Lobule VI, VIIB, and Crus I are involved explicitly in executive functions, including working memory, planning, organizing, and strategy formation, all of which are important for divergent creative thinking [28– 31]. The left lobule VI, VIIB, Crus I, and Crus II of the cerebellum are significantly associated with Visual activity and Visual divergent thinking such as photography, and drawing[32]. Comparing hallucinators to controls across both groups(Charles Bonnet Syndrome and Parkinson's disease), lower GMV(grey matter volume) was found within cerebellar lobule VIIIb、VIIIa、IX、VIIb. Predominantly within PD[33].

Cortico-cerebellar FC objective manifestations occur in PD patients, and the characteristics and differences of cerebellar FC in PD-H, PD-NH, and HC remain. This study validated the effectiveness of cortico-cerebellar as a feature in a classification task across all subjects using SVM. The sensitivity and specificity of the classifiers were also evaluated for various tasks and the confidence intervals for each result.

2. Materials and Methods

2.1. Participants

All study subjects were recruited from the Nanjing Brain Hospital between November 2018 to October 2022. All subjects were right-handed, and included 17 PD-H subjects (9 males and 8 females), 13 PD-NH subjects (5 males and 8 females), and 26 HC were not different statistically in terms of age and sex (12 males and 14 females). Diagnostic criteria for Parkinson's disease in China (2016 edition) The inclusion criteria for HC included: 1) no current cognitive problems, 2) no neurological or psychiatric disorders, and 3) a clinical dementia score of 0. All participants provided written informed consent, and the study was approved by the Medical Research Ethical Committee of Nanjing Brain Hospital in Nanjing, China.

2.2. Magnetic Resonance Imaging Data Acquisition

Magnetic resonance imaging (MRI) was acquired utilizing a Siemens 3.0 T singer scanner (Siemens, Verio, Germany) with an 8-channel radio frequency coil at the Affiliated Brain Hospital of Nanjing Medical University. Participants were asked to remain as still as possible, close their eyes, remain awake, and not think of anything. T1WI was acquired by applying a three-dimensional magnetization prepared rapid gradient echo (3D-MPRAGE). The parameters included time repetition (TR) = 2,530 ms, echo time (TE) = 2.48 ms, inversion time (TI) = 1100 ms, number of slices =

 doi:10.20944/preprints202309.1618.v1

176, thickness = 1 mm, gap = 0.5 mm, matrix = 256 × 256, flip angle (FA) =90^0, field of view (FOV) = 256 × 256 mm, and voxel size = 1 × 1 × 1 mm^3. Resting-state fMRI acquisition was applied using single echo planar imaging (EPI). The gradient echo-echo planar imaging (GRE-EPI) sequence included 240 time points. TE = 30 ms; TR = 2000 ms; number of slices = 31, FOV = 220 × 220 mm^2; matrix = 64 × 64; FA =90^0; thickness = 4 mm, gap = 0 mm. The imaging for each subject took ~14 min.

2.3. Data Preprocessing

The fMRI data were processed using the Data Processing and Analysis for Brain Imaging (DPABI, http://www.rest.restfmri.net) [34]. The first 10 volumes of the rest session were discarded for each subject. The remaining images were corrected utilizing slice timing and motion (head motion ≤3 mm, head motion angle ≤3^0). Next, resting-state fMRI images were co-registered to high-resolution 3D-T1 structural images. Normalization of 3D-T1 structural MRI images to Montreal Neurological Institute (MNI) space was undertaken via non-linear warping based on Diffeomorphic Anatomical Registration Through Exponentiated Lie Algebra (DARTEL). After spatial normalization to T1 space, all images were resampled into 3 × 3 × 3 mm^3 voxels and spatially smoothed using a Gaussian filter of 6 mm full-width at half-maximum (FWHM). Data was then temporally bandpass-filtered (0.01–0.08 Hz) to eliminate low-frequency drifts and physiological high-frequency noise. Furthermore, to reduce the confounding artifacts of resting head movements and physiological noise (respiration and cardiac fluctuations), nuisance covariates were regressed, including the Friston 24-motion parameter model, global mean, white matter, and cerebrospinal fluid signals.

2.4. Functional Connectivity Analysis

From the perspective of structural anatomy, the bilateral cerebellar(26 regions) can be divided into cerebellum(26 regions) and vermis(8 regions) shown in Figure.1, were extracted as seed regions of interest (ROI) utilizing the DPABI software package template (anatomical automatic labeling, AAL). FC analysis was performed between each seed region and the whole brain(115 regions), in a voxel-wise manner using the DPABI software. The voxels of each seed region of every subject were extracted and averaged to obtain the reference time series of seed points. Then, we calculated the correlation coefficient between the reference time series and the time series involving all other brain voxels. This part obtained 2990 connectivity features (115 * 26 = 2990).

2.5. Feature Select

The correlation coefficients were transformed into z-values using the Fisher r-to-z transformation, improving normality to improve the classification performance of machine learning. All data were tested for normality and variance congruence. One-way ANOVA tests were performed to compare the FC values across groups (PD-H, PD-NH, and HC).

We then used post-hoc multiple comparisons to compare results between pairs of groups. We considered $p < 0.05$ as statistically significant in our dataset which was used as a training feature in classification task. FC with a p-value<0.001 is considered statistically significant and will be discussed in this article.

Three features were selected for training separately: Feature.1 all cortico-cerebellar FC; Feature.2, all ROI seed sequences with significance in the Statistical Analysis; Feature.3 cortico-cerebellar FC with significance in the analysis. In the classification task, since only Feature.1 was consistent across the three groups of subjects, three sets of binary classification tasks were set: PD-H versus(vs). PD-NH, PD-H vs. HC, and PD-NH vs. HC.

Preprints (www.preprints.org) | NOT PEER-REVIEWED | Posted: 25 September 2023 doi:10.20944/preprints202309.1618.v1

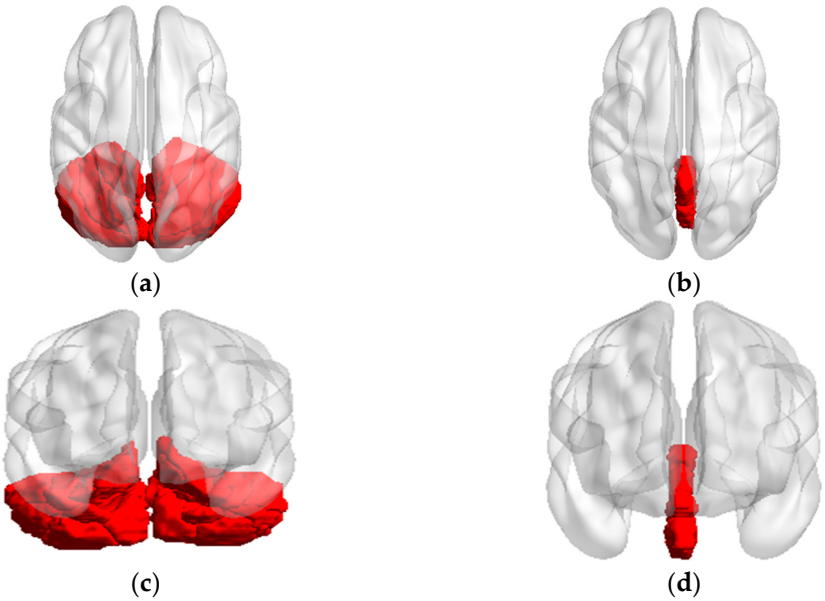

Figure 1. The axial and conronal sight of seed regions (a) Axial sight of cerebellm; (b) Axial sight of vermis; (c) Coronal sight of cerebellm; (d) Coronal sight of vermis.

2.6. SVM classification

The SVM was implemented in MATLAB (The Math Works, Natwick, MA) and LIBSVM (http://www.csie.ntu.edu.tw/ cjlin/libsvm/). The kernel function in the SVM classifier uses the radial basis kernel function (RBF), where the penalty parameter C and the kernel bandwidth s in the kernel function range from $[4^{-4},4^{4}]$. The RBF kernel was defined as follows:

$$\mathrm{K}(x_1, x_2) = \exp\left(-\|x_1 - x_2\|/(2\sigma^2)\right) \quad (1)$$

where x_1, x_2 are two eigenvectors, σis the width parameter of the REF kernel.

A 4-fold cross-validation approach was used to assess the models by training four models for each experiment. In each iteration, 75% of the data were randomly selected for training and 25% for testing. Thus, this process results in one prediction per sample of the entire dataset. This process was repeated four times to assess the variability of the evaluation metrics.

In cross-validation, the optimal model result in the testing set is recorded as the classification accuracy under this task. The test set consists of two parts of data: one is the training data of the optimal model summed with the white noise of level 10^{-3}, and the other is the test data in the training of the optimal model. Metrics of model performance were accuracy (percent correctly classified) and area under the receiver operating characteristics (ROC-AUC) curve.

Finally, the held-out sample was used to evaluate the training classifier. These parameters were defined as follows:

$$\mathrm{Accurary(ACC)} = (TP + TN)/(TP + TN + FP + FN) \quad (2)$$

where TP is true positive, TN is true negative; FP is false positive, and FN is false negative, respectively. Area Under Curve (AUC) was defined as the area under the ROC curve and the coordinate axis.

$$\mathrm{Sensitivity(SEN)} = TP/(TP + FN), \quad \mathrm{Specificity(SPE)} = TP/(TP + FN) \quad (3)$$

The 95% confidence intervals (CIs) of ACC, SEN, and SPE were calculated by the exact Clopper–Pearson method.

3. Results

3.1. Functional Connectivity Changes of the cerebellar

Preprints (www.preprints.org) | NOT PEER-REVIEWED | Posted: 25 September 2023 doi:10.20944/preprints202309.1618.v1

The results of the FC Statistical Analysis with p-value<0.001 for the three populations are recorded in Table 1, with the significantly different FC connections in each of the two groups of subjects in the form of x vs. y. Node a is the cerebellar ROI as seed, and Node-b is the node connected to Node-a. The brain regions in the table are recorded with the names in the AAL template. Abnormal FC connections are shown in Figure.2

The FC connections with p-value<0.05 were shown in Supplementary Table 1 in Appendix A, Not discussed in this article, interested readers can refer to it.

Table 1. FC statistical analysis results for p<0.001.

PD-H vs HC		PD-H vs PD-NH	
Node-a	**Node-b**	Node-a	Node-b
Vermis_4_5	Precuneus_L	Vermis_1_2	Frontal_Inf_Oper_L Frontal_Inf_Oper_R Frontal_Inf_Tri_L Frontal_Inf_Tri_R Postcentral_L Parietal_Inf_L Precuneus_L
PD-NH vs HC			
Vermis_1_2	Frontal_Inf_Oper_L Frontal_Inf_Tri_L Cerebelum_4_5_L		

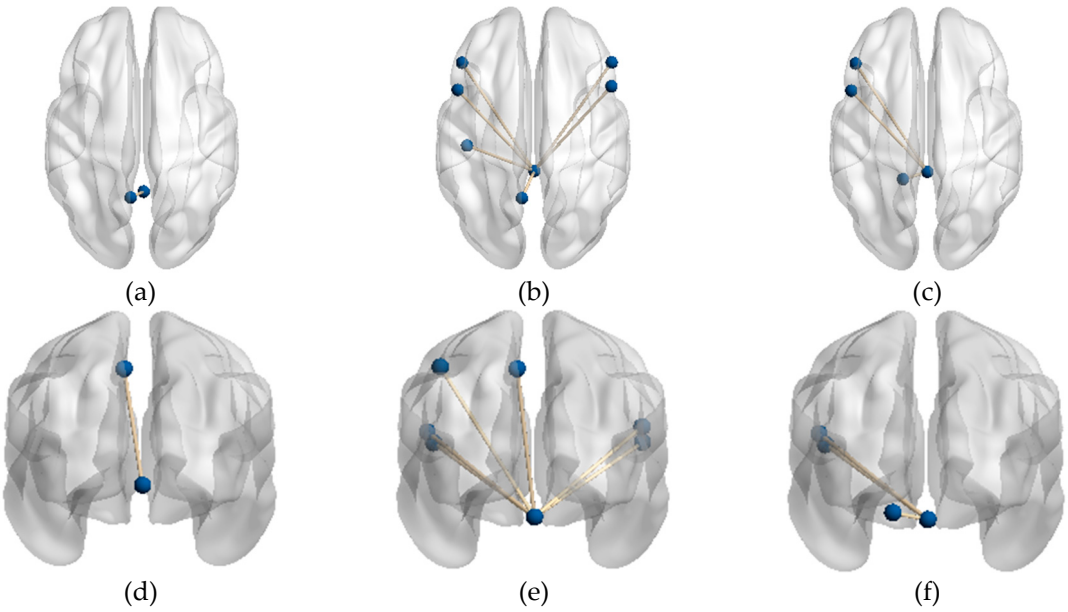

Figure 2. FC connections with significant differences (a) Axial sight of FC between the PD-H and HC groups; (b) Axial sight of FC between the PD-H and PD-NH groups; (c) Axial sight of FC between the PD-NH and HC groups; (d) Coronal sight of FC between the PD-H and HC groups; (e) Coronal sight of FC between the PD-H and PD-NH groups; (f) Coronal sight of FC between the PD-NH and HC groups.

3.1.1. Functional Connectivity Changes of the Vermis Lobule I_II

In comparison to PD-NH, the FC value between vermis lobule I_II and frontal lobe/ bilateral IFGoprec, bilateral IFCtriang, left parietal lobe/ PreCG, PoCG, and IPL were remarkably increased in the PD-H group.

Also, FC values in vermis lobule I_II and left frontal lobe/IFGoprec, IFCtriang, left side of cerebellum lobule IV were significantly increased in HC compared to the PD-NH group.

Preprints (www.preprints.org) | NOT PEER-REVIEWED | Posted: 25 September 2023 doi:10.20944/preprints202309.1618.v1

3.1.2. Functional Connectivity Changes of the Vermis Lobule IV_V

In comparison to HC, the FC value between vermis lobule IV_V and left parietal lobe/ PreCG were remarkably increased in the PD-H group. There were no significant differences in FC values of vermis lobule IV_V and whole brain between other groups.

3.2. Machine learning training results

The training results of cerebellar features for the three populations are shown in Table 2, where the training results of Feature.1, Feature.2, and Feature.3 are recorded respectively.

The average result of k-fold cross-validation for each group of records and the ROC curve coverage area AUC of the corresponding models. The CI interval for each result value is recorded in [] form next to that value.

Table 2. Feature training results.

	ACC	SEN	SPE	AUC
Feature.1				
PD-H:HC	93.02 [80.94,98.54]	88.24 [63.56,98.54]	96.15 [80.36,99.90]	0.9910
PD-H:PD-NH	86.67 [69.28,96.24]	88.24 [63.56,98.54]	84.62 [54.55,98.08]	0.9819
PD-NH:HC	92.31 [79.13,98.38]	84.62 [54.55,98.08]	96.15 [80.36,99.90]	0.9970
Ferutre.2				
PD-H:HC	88.37 [74.92,96.11]	82.35 [56.57,92.30]	92.31 [74.87,99.05]	0.9140
PD-H:PD-NH	93.33 [77.93,99.18]	94.12 [71.31,99.85]	92.31 [63.97,99.81]	0.9955
PD-NH:HC	89.74 [75.78,97.13]	92.31 [63.97,99.81]	88.46 [69.85,97.55]	0.9527
Feature.3				
PD-H:HC	74.42 [58.83,86.48]	70.59 [44.04,84.69]	76.92 [56.35,91.03]	0.7715
PD-H:PD-NH	80.00 [61.43,92.29]	88.24 [63.56,98.54]	69.23 [38.57,90.91]	0.9186
PD-NH:HC	89.47 [75.78,97.13]	92.31 [63.97,99.81]	88.46 [69.85,97.55]	0.9349

In the classification tasks for PD-H and HC, the model of Feature.1 has the highest accuracy, and Feature.1 is more sensitive to HC. In the classification task for PD-H and PD-NH, the model of Feature.2 has the highest accuracy, and the model is optimal in all parameters.

In the classification task for PD-NH and HC, the model of Feature.1 has the highest model accuracy with the highest AUC and is more sensitive to HC, Feature.2 and Feature.3 are more sensitive to PD-NH. Figure.3 shows the ROC curves of the Feature.1, Fearure.2 and Feature.3 training models for the three sets of tasks.

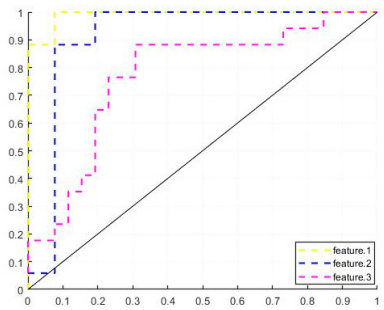

(a)

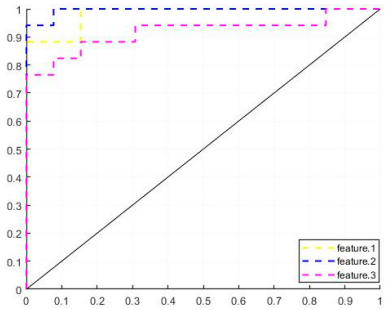

(b)

Preprints (www.preprints.org) | NOT PEER-REVIEWED | Posted: 25 September 2023 doi:10.20944/preprints202309.1618.v1

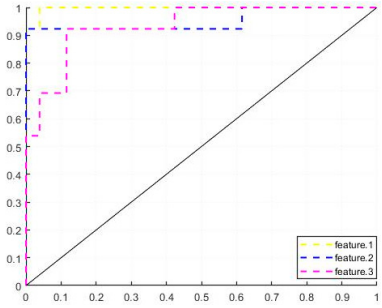

(c)

Figure 3. ROC curves (a) Feature.1; (b)Feature.2; (c)Feature.3.

4. Discussion and Conclusions

In the present study, alterations in FC between the cerebellum and whole brain were investigated among subjects with PD-H, PD-NH, and HC. We designed three groups of cerebellar features for machine learning training to classify three groups of subjects and achieved good classification results. We also explored the relevance of this change to visual hallucination.

The current research indicates that there are significant changes in the FC of cerebellar cognitive subregions within the PD-H groups. The research on brain functional connections of PD-H is now a hot topic[35], but few studies have evaluated the effect of cerebellum function connections.

4.1. Functional Connectivity Changes in the PD-H patients

In the present study, changed FC in the PD-H group in Table 1 were mainly in VLPFC, included the right side of IFGoprec and IFCtriang, DMN including the left side of PoCG, IPL, and PCUN.

DMN is a brain resting network that is activated when individuals are not engaged in attending to or responding to external stimuli and are involved in regulating self-reflection and memory processes[36-38], which may cause hallucinations.

Previous studies have shown that interruptions in DMN and its internal functional connections are the basis for mild hallucinations in PD[39]. Furthermore, a strong relationship between DMN, lobule IX, and crus II has been reported previously[40]. In this study, it was found that compared to the PD-NH, the FC connection between PD-H cerebellar vermis and DMN was also significantly increased. Thus, increased cerebellar function connectivity to the DMN network in PD-H patients may be one of the causes involved in visual hallucination.

In the comparison of PD-H and HC, only the connection between Vermis_4_5 and the left side of PCUN was significant in the FC with $p<0.001$ in Table 1, which also appeared in the group comparison between PD-H and PD-NH means the left side of PCUN is a common brain area that frequently interacts with the cerebellum in PD-H patients.

PCUN is a part of the posterior parietal cortex, located in the inner hemisphere of the brain, and is an important brain area in DMN. Its cognitive function involves situational memory, visual space, self-related information processing, as well as metacognition, consciousness, and other processes. It is an advanced cognitive ability for individuals to evaluate their memory accuracy.

Some research has also shown that more active PCUN allows more information to flow in the brain, connecting unrelated things. When schizophrenia patients perform memory tasks, they have less inhibition of PCUN. Therefore, the generation of visual hallucinations may also be a result of memory dysfunction, in which the cerebellum also participates in related regulation.

For the enhanced connectivity between Vermis_1_2 and VLPFC in the PD-H group, in the Domain-Specific hypothesis[41], VLPFC primarily controls visuospatial and shape information, transferring this information to each other through parallel loops in other brain regions, allowing both types of information to be represented in the dorsolateral and ventral lateral prefrontal cortex. Over-activation of connectivity in the PD-H group leads to an imbalance of visual information across brain regions and thus to hallucinations, a process in which the cerebellar vermis is also involved.

4.2. Functional Connectivity Changes in the PD-NH patients

The primary node of cerebellar abnormality in the PD-NH group subjects compared with the other two groups was Vermis_1_2, and both showed significant reduction.

In the comparison of PD-NH and HC, the connection between Vermis_1_2 and the left side of IFGoprec, IFCtriang, and cerebellar lobule IV_V was significant in the FC with $p<0.01$ in Table 1. These brain regions are mainly responsible for motor functions, and the weakened cerebellar connections to its FC may be associated with motor deficits in PD patients.

4.3. Functional Connectivity Changes in the PD-NH patients

In the classification task of PD-H versus HC, the model ACC gradually decreased with the reduction of cerebellar FC connections, indicating that multiple groups of cerebellar FC connections occurred abnormally and with classification sensitivity in PD-H compared to the HC. The model was more sensitive to the HC subjects, with a screening rate of 96.15%, while it reached only 88.24% for PD-H. The model accuracy decreases significantly in the training of Feature.3, probably due to the low number of FC connections with significance.

In the classification task of PD-H versus PD-NH, the model's ACC obtained optimal results in Feature.2, indicating that the cerebellar vermis of the two groups of subjects produces different directions of modulation of the brain compared to each other, and the inclusion of FC connections of other cerebellum decreases the classification sensitivity of this feature. The model is more sensitive to PD-H subjects, with a screening rate of 94.12%.

In the classification task of PD-NH with HC, the model ACC obtained the best results in Feature.1. The classification effect of the models trained with Feautre.2 and Feautre.3 was identical. However, the model AUC was still higher for Feautre.2, which means the added features in Feauture.2 compared to Feauture.3 still had an enhancement effect.

Cerebellar FC connections performed best in the classification task of Feature.1, indicating that most cerebellar FC connections were also changed in PD-H and PD-NH, but some of the changes are not significant enough at the moment but can be identified and exploited by the SVM model.

5. Conclusions

In previous studies of Parkinson's hallucinations, the mechanism of hallucination production has often focused on the brain, but this study shows that the cerebellum is a neglected point. Cerebellum Vermis has been thought to be associated with motor regulation, but based on experimental results, it appears to be closely linked to the DMN network and has an important role in hallucination-related cognitive regulation, which may be an important brain region that has been overlooked in previous studies.

6. Patents

Author Contributions: Conceptualization, Liangcheng Qu, Kuiying Yin, Weiguo Liu and JingPing Shi; Data curation, Liangcheng Qu and Yiting Cao; Formal analysis, Liangcheng Qu and Chuan Liu; Funding acquisition, Kuiying Yin and Weiguo Liu; Investigation, Liangcheng Qu; Methodology, Liangcheng Qu, Chuan Liu, JingPing Shi, Kuiying Yin and Weiguo Liu; Project administration, Liangcheng Qu, Kuiying Yin and Weiguo Liu; Software, Liangcheng Qu; Supervision, JingPing Shi, Kuiying Yin and Weiguo Liu; Validation, Liangcheng Qu and Yiting Cao; Writing – original draft, Liangcheng Qu; Writing – review & editing, Liangcheng Qu, Weiguo Liu, Kuiying Yin and JingPing Shi. All authors will be informed about each step of manuscript processing including submission, revision, revision reminder, etc. via emails from our system or assigned Assistant Editor.

Funding: This research was funded by the National Natural Science Foundation of China, grant number U19B2018.

Institutional Review Board Statement: The study was conducted according to the guidelines of the Declaration of Helsinki, and approved by the Ethics Committee of the Affiliated Brain Hospital of Nanjing Medical University (2022-KY132-01， approved date: 22 July 2022).

Informed Consent Statement: Informed consent was obtained from subjects involved in the study.

Data Availability Statement: The data are available upon reasonable request.

Acknowledgments: We would like to thank Rumei Li for their help in collecting data, Wendu Tao, and Chao Yu for their suggestions on data processing.

Conflicts of Interest: The authors declare that there is no conflict of interest regarding the publication of this paper.

Appendix A

Supplementary Table 1 FC statistical analysis results for p<0.05

PD-H vs HC		PD-H vs PD-NH	
Node-a	Node-b	Node-a	Node-b
Cerebelum_3_R	Frontal_Mid_R		
Cerebelum_4_5_L	Precuneus_L		
Cerebelum_4_5_R	Occipital_Inf_R		
	Precuneus_L		
Cerebelum_6_R	Postcentral_L		
	Precuneus_L		Precentral_L
Cerebelum_9_L	Occipital_Inf_R		Frontal_Mid_L
Cerebelum_9_R	Frontal_Sup_R		Frontal_Inf_Oper_L
	Frontal_Mid_R		Frontal_Inf_Oper_R
	Occipital_Inf_R		Frontal_Inf_Tri_L
	Postcentral_L	Vermis_1_2	Frontal_Inf_Tri_R
	Parietal_Inf_L		Cingulum_Mid_R
	Precuneus_L		Postcentral_L
	Temporal_Sup_L		Parietal_Inf_L
Vermis_3	Frontal_Mid_R		Precuneus_L
Vermis_1_2	Occipital_Inf_R		Precuneus_R
Vermis_4_5	Occipital_Inf_R		
	Postcentral_L		
	Parietal_Inf_L		
	Precuneus_L		
Vermis_8	Occipital_Inf_R		
PD-NH vs HC			
Cerebelum_9_R	Temporal_Sup_L		
Vermis_1_2	Precentral_L		
	Frontal_Inf_Oper_L		
	Frontal_Inf_Oper_R		
	Frontal_Inf_Tri_L		
	ParaHippocampal_L		
	Angular_R		
	Cerebelum_4_5_L		
	Cerebelum_4_5_R		

References

1. Sveinbjornsdottir S. The clinical symptoms of Parkinson's disease[J]. J Neurochem,2016, 139 Suppl 1: 318-324.
2. Pfeiffer R F. Non-motor symptoms in Parkinson's disease[J]. Parkinsonism RelatDisord, 2016, 22 Suppl 1: S119-22.
3. Martinez-Martin P, Schapira A H, Stocchi F, et al. Prevalence of nonmotor symptoms in Parkinson's disease in an international setting; study using nonmotor symptoms questionnaire in 545 patients[J]. Mov Disord, 2007, 22(11): 1623-9.

4. Chaudhuri K R, Martinez-Martin P, Schapira A H, et al. International multicenter pilot study of the first comprehensive self-completed nonmotor symptoms questionnaire for Parkinson's disease: the NMSQuest study[J]. Mov Disord, 2006, 21(7): 916-23.
5. Guo Y, Xu W, Liu F T, et al. Modifiable risk factors for cognitive impairment in Parkinson's disease: A systematic review and meta-analysis of prospective cohort studies[J]. Mov Disord, 2019, 34(6): 876-883.
6. Dehsarvi A . Classification of resting-state fMRI using evolutionary algorithms : towards a brain imaging biomarker for Parkinson's disease[J]. University of York, 2018.
7. Gwenda, Engels, Annemarie, et al. Dynamic Functional Connectivity and Symptoms of Parkinson's Disease: A Resting-State fMRI Study.[J]. Frontiers in Aging Neuroscience, 2018.
8. Bejr-Kasem H, Pagonabarraga J, Martínez-Horta S, et al. Disruption of the default mode network and its intrinsic functional connectivity underlies minor hallucinations in Parkinson's disease[J]. Mov Disord, 2019, 34(1): 78-86
9. Holroyd S, Wooten GF. Preliminary FMRI evidence of visual system dysfunction in Parkinson's disease patients with visual hallucinations[J]. Neuropsychiatry Clin Neurosci, 2006, 18(3): 402-404
10. Yao N, Shek-Kwan Chang R, Cheung C, et al. The default mode network is disrupted in Parkinson's disease with visual hallucinations[J]. Human Brain Mapping, 2014, 35(11): 5658-5666
11. Rapoport M, van Reekum R, Mayberg H. The role of the cerebellum in cognition and behavior: a selective review[J]. Neuropsychiatr Clin Neurosci. (2000) 12:193–8. doi: 10.1176/jnp.12.2.193
12. Schmahmann JD, Caplan D. Cognition, emotion and the cerebellum. Brain[J].(2006) 129(Pt 2):290–2. doi: 10.1093/brain/awh729
13. Balsters JH, Whelan CD, Robertson IH, Ramnani N. Cerebellum and cognition: evidence for the encoding of higher order rules[J]. Cereb Cortex.(2013) 23:1433–43. doi: 10.1093/cercor/bhs127
14. Fan L, Hu J, Ma W, Wang D, Yao Q, Shi JJN, et al. Altered baseline activity and connectivity associated with cognitive impairment following acute cerebellar infarction: a resting-state fMRI study[J]. Neurosci Lett. (2019) 692:199–203. doi: 10.1016/j.neulet.2018.11.007
15. Wang D, Yao Q, Yu M, Xiao C, Fan L, Lin X, et al. Topological disruption of structural brain networks in patients with cognitive impairment following cerebellar infarction[J]. Front Neurol. (2019), 10:759. doi: 10.3389/fneur.2019.00759
16. Schmahmann JD, Sherman JC. The cerebellar cognitive affective syndrome.Brain[J]. (1998) 121 (Pt 4):561–79. doi: 10.1093/brain/121.4.561
17. Hoche F, Guell X, Vangel MG, Sherman JC, Schmahmann JD. The cerebellar cognitive affective/Schmahmann syndrome scale[J]. Brain. (2018) 141:248–70. doi: 10.1093/brain/awx317
18. Ahmadian N, van Baarsen K, van Zandvoort M, Robe PA. The cerebellar cognitive affective syndrome-a meta-analysis[J]. Cerebellum. (2019) 18:941–50. doi: 10.1007/s12311-019-01060-2
19. Sereno MI, Diedrichsen J, Tachrount M, Testa-Silva G, d'Arceuil H, De Zeeuw. C. The human cerebellum has almost 80% of the surface area of the neocortex[J]. Proc Natl Acad Sci USA. (2020) 117:19538–43. doi: 10.1073/pnas.2002896117
20. Lawn T , Ffytche D . Cerebellar Correlates of Visual Hallucinations in Parkinson's Disease and Charles Bonnet Syndrome[J]. Cortex, 2020.
21. Buckner RL, Krienen FM, Castellanos A, Diaz JC, Yeo BT. The organization of the human cerebellum estimated by intrinsic functional connectivity[J]. Neurophysiol. (2011) 106:2322–45. doi: 10.1152/jn.00339.2011
22. Toniolo S, Serra L, Olivito G, Caltagirone C, Mercuri N, Marra C, et al. Cerebellar white matter disruption in Alzheimer's disease patients: a diffusion tensor imaging study[J]. (2020) 74:615 24. doi: 10.3233/JAD-191125
23. Zhang L, Ni H, Yu Z, Wang J, Qin J, Hou F, et al. Investigation on the alteration of brain functional network and its role in the identification of mild cognitive impairment[J]. Front Neurosci. (2020) 14:558434. doi: 10.3389/fnins.2020.558434
24. Bai F, Liao W, Watson DR, Shi Y, Yuan Y, Cohen AD, et al. Mapping the altered patterns of cerebellar resting-state function in longitudinal amnestic mild cognitive impairment patients[J]. Alzheimers Dis. (2011) 23:87–99. doi: 10.3233/JAD-2010-101533
25. Sveljo O, Culic M, Koprivsek K, Lucic M. The functional neuroimaging evidence of cerebellar involvement in the simple cognitive task[J]. Brain Imaging Behav. (2014) 8:480–6. doi: 10.1007/s11682-014-9290-3
26. Kuper M, Kaschani P, Thurling M, Stefanescu MR, Burciu RG, Goricke S, et al. Cerebellar fMRI activation increases with increasing working memory demands[J]. Cerebellum. (2016) 15:322–35. doi: 10.1007/s12311-015-0703-7
27. Schmahmann JD. Cerebellum in Alzheimer's disease and frontotemporal dementia: not a silent bystander[J]. Brain. (2016) 139(Pt 5):1314–8. doi: 10.1093/brain/aww064
28. Stoodley CJ, Schmahmann JD. Functional topography in the human cerebellum: a meta analysis of neuroimaging studies[J]. Neuroimage. (2009) 44:489–501. doi: 10.1016/j.neuroimage.2008.08.039

29. Sokolov AA, Miall RC, Ivry RB. The cerebellum: adaptive prediction for movement and cognition[J]. Trends Cogn Sci. (2017) 21:313–32. doi: 10.1016/j.tics.2017.02.005
30. Guell X, Gabrieli JDE, Schmahmann JD. Triple representation of language, working memory, social and emotion processing in the cerebellum: convergent evidence from task and seed-based restingstate fMRI analyses in a single large cohort[J]. Neuroimage. (2018) 172:437–49. doi: 10.1016/j.neuroimage.2018.01.082
31. Shipman ML, Green JT. Cerebellum and cognition: does the rodent cerebellum participate in cognitive functions?[J]. Neurobiol Learn Mem. (2019) 106996. doi: 10.1016/j.nlm.2019.02.006
32. Gao Z, Liu X, Zhang D, Liu M, Hao N. The indispensable role of the cerebellum in visual divergent thinking[J]. Sci Rep. (2020) 10:16552. doi: 10.1038/s41598-020-73679-9
33. Lawn T , Ffytche D .Cerebellar Correlates of Visual Hallucinations in Parkinson's Disease and Charles Bonnet Syndrome[J].Cortex, 2020.DOI:10.1016/j.cortex.2020.10.024.
34. Yan CG, Wang XD, Zuo XN, Zang YF. DPABI: data processing and analysis for (Resting-State) brain imaging[J]. Neuroinformatics. (2016) 14:339–51. doi: 10.1007/s12021-016-9299-4
35. Hepp DH, Foncke EMJ, Olde Dubbelink KTE, et al. Loss of functional connectivity in patients with parkinson disease and visual hallucinations[J]. Radiology, 2017, 285(3): 896-90
36. Raichle ME. The brain's default mode network[J]. Annu Rev Neurosci. (2015) 38:433–47. doi: 10.1146/annurev-neuro-071013-014030
37. Davey CG, Pujol J, Harrison BJ. Mapping the self in the brain's default mode network[J]. Neuroimage. (2016) 132:390–7. doi: 10.1016/j.neuroimage.2016.02.022
38. Davey CG, Harrison BJ. The brain's center of gravity: how the default mode network helps us to understand the self. World Psychiatr[J]. (2018) 17:278–9. doi: 10.1002/wps.20553
39. Bejr-kasem, Helena, Pagonabarraga J ,Martínez-Horta, Saül,et al.Disruption of the default mode network and its intrinsic functional connectivity underlies minor hallucinations in Parkinson's disease[J].Movement Disorders, 2018.DOI:10.1002/mds.27557.
40. Habas C, Kamdar N, Nguyen D, et al. Distinct cerebellar contributions to intrinsic connectivity networks[J]. Neurosci, 2009, 29:8586–94.
41. Junghee,Kim,Jeong,et al.The Effect of Memory Load on Maintenance in Face and Spatial Working Memory: An Event-Related fMRI Study[J].KOREAN JOURNAL OF COGNITIVE SCIENCE, 2010, 21(2):359-386.